

High-Throughput Screening for Small-Molecule Activators of Neutrophils: Identification of Novel *N*-Formyl Peptide Receptor Agonists^[S]

Igor A. Schepetkin, Liliya N. Kirpotina, Andrei I. Khlebnikov, and Mark T. Quinn

Department of Veterinary Molecular Biology, Montana State University, Bozeman, Montana (I.A.S., L.N.K., M.T.Q.); and Department of Chemistry, Altai State Technical University, Barnaul, Russia (A.I.K.)

Received December 4, 2006; accepted January 17, 2007

ABSTRACT

We screened a chemolibrary of drug-like molecules for their ability to activate reactive oxygen species (ROS) production in murine phagocytes, and we identified 26 novel compounds with potent neutrophil activating properties. We used substructure screening, fragment-focusing, and structure-activity relationship analyses to further probe the parent library and defined at least two groups of activators of ROS production in murine neutrophils: *t*-butyl benzene and thiophene-2-amide-3-carboxylic ester derivatives. Further studies of the active compounds revealed 11 compounds that activated ROS production in human neutrophils, and six of these compounds also activated intercellular Ca^{2+} mobilization and chemotaxis in human neutrophils. Of the latter compounds, compound **14** (1,3-benzodioxolane-5-carboxylic acid 4'-benzyloxy-3'-methoxybenzylidene-hydrazide) activated neutrophils at nanomolar concentrations, and Ca^{2+} mobilization was inhibited by pertussis toxin and *N*-*t*-butoxycarbonyl-Phe-Leu-Phe-Leu-Phe (Boc-2), an antagonist of formyl peptide receptors (FPR/FPRL1).

Likewise, activation by compound **14** was desensitized after *N*-formyl-Met-Leu-Phe pretreatment. Similar biological activities were found for compound **104** (1,3-benzodioxolane-5-carboxylic acid 3'-bromo-5'-ethoxy-4'-hydroxybenzylidenehydrazide), an analog of compound **14**. Furthermore, conformational analysis of the activators of chemotaxis and Ca^{2+} mobilization showed a high degree of similarity in distances between pharmacophore points of compounds **14** and **104** with a model of FPR published by Edwards et al. (*Mol Pharmacol* **68**:1301–1310, 2005), indicating that conformational features of the agonists identified here are structurally compatible with steric constraints of the ligand-binding pocket of the receptor. Based on these results, we conclude that compounds **14** and **104** represent novel small-molecule agonists of FPR. These studies enhance our understanding of FPR ligand/receptor interactions and structure/activity relationships of phagocyte agonists.

The host defense response of humans is complex and involves many cell types with distinct but overlapping roles (Beutler, 2004). One of the earliest cell types responding to invasion by potentially pathogenic organisms are phago-

cytes, which are key participants in the innate immune response (Beutler, 2004). These cells perform a variety of complex microbicidal functions, including chemotaxis, phagocytosis, and destruction of targeted organisms (Witko-Sarsat et al., 2000). Indeed, the spectrum of microorganisms kept in check by phagocytes includes fungi, bacteria, and virus-infected cells (Witko-Sarsat et al., 2000).

Phagocytes can be activated by a wide variety of stimuli, including cytokines and other endogenous chemical messengers, pathogen-associated molecular structures, and oligopeptides derived from various pathogens or produced endogenously (Beutler et al., 2003; Guo and Ward, 2005). In addition, novel phagocyte agonists have been identified by screening cultured cell lines transfected with specific recep-

This work was supported in part by Department of Defense grant W9113M-04-1-0001, National Institutes of Health grants AR042426 and RR020185, and the Montana State University Agricultural Experimental Station.

The U.S. Army Space and Missile Defense Command, 64 Thomas Drive, Frederick, MD 21702 is the awarding and administering acquisition office. The content of this report does not necessarily reflect the position or policy of the U.S. Government.

Article, publication date, and citation information can be found at <http://molpharm.aspetjournals.org>.
doi:10.1124/mol.106.033100.

[S] The online version of this article (available at <http://molpharm.aspetjournals.org>) contains supplemental material.

ABBREVIATIONS: ROS, reactive oxygen species; SAR, structure-activity relationship; DMSO, dimethyl sulfoxide; HRP, horseradish peroxidase; fMLF, *N*-formyl-Met-Leu-Phe; PMA, phorbol 12-myristate 13-acetate; PTX, pertussis toxin; IL-8, interleukin-8; HBSS, Hanks' balanced salt solution; GPCR, G protein-coupled receptor; FPR, formyl peptide receptor; FPRL1, formyl peptide receptor like 1; MK-886, 3-[3-butylsulfanyl-1-[(4-chlorophenyl)methyl]-5-propan-2-yl-indol-2-yl]-2,2-dimethyl-propanoic acid; Boc-2, *N*-*t*-butoxycarbonyl-Phe-Leu-Phe-Leu-Phe; CXCR2, CXC chemokine receptor 2.

tors to identify new receptor ligands. This highly specific method has revealed agonists to receptors for granulocyte colony-stimulating factor (Tian et al., 1998), *N*-formyl peptides (Nanamori et al., 2004), C3a (Mathieu et al., 2005), and C5a (Buck and Wells, 2005). However, this approach is somewhat restricted by the limited availability of known receptor targets, and agonists identified with cell lines often respond differently in functional testing with primary cell targets (Buck and Wells, 2005; Mathieu et al., 2005). Primary phagocytes have also been used in screening for novel agonists, and this approach led to the identification of a number of small molecules that induce interferon- α in macrophages and may be agonists of Toll-like receptor 7/8 (Fletcher et al., 2006). Likewise, Bae et al. (2003) identified an activator of phospholipase C using primary high-throughput screening that was based on measurement of reactive oxygen species (ROS) production by human neutrophils. In most other reports on this topic, phagocyte-activating properties have primarily been reported as side-effects of various drugs (for review, see Labro, 2000). For example, several cephalosporin antibiotics have been shown to stimulate neutrophils (Scheffer et al., 1992), and it has been suggested that enhancement of phagocyte function may contribute to the antibacterial action of these antibiotics. Phagocytes can also be activated by non-steroidal anti-inflammatory drugs, which is potentially a negative or pro-inflammatory side effect of these drugs (Fiorucci et al., 1997).

The wide range of unrelated substances with phagocyte-activating properties suggests the possibility that compounds or drugs from different pharmacological groups (or target families) could have common structural scaffold(s) associated with phagocyte activation. Furthermore, determination of these privileged structures would not only enhance our understanding of the structure/activity relationships of known phagocyte activators but might also lead to the development of novel phagocyte agonists. To address this issue, we screened a diverse library of drug-like molecules in an effort to identify novel compounds that stimulate neutrophil functional activity and used molecular modeling methods to analyze structural features of these agonists.

Screening of a 10,000-molecule chemolibrary resulted in the identification of several compounds that activated neutrophil ROS production at low micromolar concentrations. Further substructure screening, fragment-focusing, and structure-activity relationship (SAR) analysis of the parent library revealed at least two groups of neutrophil activators: compounds bearing 1) a thiophene-2-amide-3-carboxylic ester scaffold or 2) a *t*-butyl benzene submolecule. One of the selected compounds activated intercellular Ca^{2+} mobilization and chemotaxis in human neutrophils at nanomolar concentrations, and the former effect was inhibited by a pertussis toxin and *N*-*t*-butoxycarbonyl-Phe-Leu-Phe-Leu-Phe (Boc-2), a specific inhibitor of FPR/FPRL1. Furthermore, compound-based pharmacophore modeling showed a high degree of similarity for several low-energy conformations of this compound and its analog to the current pharmacophore model for FPR ligands (Edwards et al., 2005). Thus, these compounds represent novel FPR agonists, which may enhance our understanding of the molecular requirements of FPR ligands.

Materials and Methods

Materials. 8-Amino-5-chloro-7-phenylpyridol[3,4-*d*]pyridazine-1,4(2*H*,3*H*)-dione (L-012) was obtained from Wako Chemicals (Richmond, VA). Dimethyl sulfoxide (DMSO), bovine superoxide dismutase, cytochrome *c*, horseradish peroxidase (HRP), *N*-formyl-Met-Leu-Phe (fMLF), Percoll, Histopaque 1077, Histopaque 1119, and phorbol 12-myristate 13-acetate (PMA) were purchased from Sigma Chemical Co. (St. Louis, MO). Pertussis toxin (PTX) and interleukin-8 (IL-8) were purchased from Calbiochem (San Diego, CA) and PeproTech Inc. (Rocky Hill, NJ), respectively. Hanks' balanced salt solution (10 \times), pH 7.4 (10 \times HBSS) (without Ca^{2+} , Mg^{2+} , and phenol red) was from Invitrogen (Carlsbad, CA). *N*-*t*-butoxycarbonyl-Phe-Leu-Phe-*D*-Leu-Phe (Boc-2) was obtained from Phoenix Pharmaceuticals (Belmont, CA). Percoll stock solution was prepared by mixing Percoll with 10 \times HBSS at a ratio of 9:1.

The chemical diversity set of 10,000 compounds was obtained from TimTec Inc. (Newark, DE). This library was randomly assembled to maximize chemical diversity with commonly accepted pharmaceutical hit structures. The compounds were diluted in DMSO at a concentration of 2 mg/ml and stored at -80°C .

Isolation of Murine Bone Marrow Leukocytes and Neutrophils. All animal use was conducted in accordance with a protocol approved by the Institutional Animal Care and Use Committee at Montana State University. Bone marrow leukocytes were flushed from tibias and femurs of BALB/c mice with HBSS, filtered through a 70- μm nylon cell strainer (BD Biosciences, Franklin Lakes, NJ) to remove cell clumps and bone particles, and resuspended in HBSS at 1×10^6 cells/ml.

Bone marrow neutrophils were isolated from bone marrow leukocyte preparations according to methods adapted from Hart et al. (1986). Bone marrow leukocytes were resuspended in 3 ml of 45% Percoll solution and layered on top of a Percoll gradient consisting of 2 ml each of 50, 55, 62, and 81% Percoll solutions in a conical 15-ml polypropylene tube. The gradient was centrifuged at 1600g for 30 min at 10°C , and the cell band located between the 61 and 81% Percoll layers was collected. The cells were washed, layered on top of 3 ml of Histopaque 1119, and centrifuged at 1600g for 30 min at 10°C to remove contaminating red blood cells. The purified neutrophils were collected, washed, and resuspended in HBSS.

Isolation of Human Neutrophils. Blood was collected from healthy donors in accordance with a protocol approved by the Institutional Review Board at Montana State University. Neutrophils were purified from the blood using dextran sedimentation, followed by Histopaque 1077 gradient separation and hypotonic lysis of red blood cells, as described previously (Gauss et al., 2005). Isolated neutrophils were washed twice and resuspended in HBSS. Neutrophil preparations were routinely >95% pure, as determined by light microscopy, and >98% viable, as determined by trypan blue exclusion.

Analysis of ROS Production. ROS production was determined by monitoring L-012-enhanced chemiluminescence, which represents a sensitive and reliable method for detecting superoxide anion (O_2^-) production in *in vitro* and *ex vivo* systems (Daiber et al., 2004). Bone marrow leukocytes were resuspended at 10^6 cells/ml in HBSS containing Ca^{2+} and Mg^{2+} (HBSS $^{++}$) and supplemented with 40 μM L-012 and 8 $\mu\text{g/ml}$ HRP. Cells (100 μl) were aliquoted into wells of 96-well flat-bottomed white microtiter plates containing test compounds diluted in 100 μl of HBSS $^{++}$ (final DMSO concentration of 1%). Luminescence was monitored for 60 min (2-min intervals) at 37°C using a Fluorescan Ascent FL microtiter plate reader (Thermo Electron, Waltham, MA). The curve of light intensity (in relative luminescence units) was plotted against time, and the area under the curve was calculated as total luminescence. The percentage activation of ROS was calculated as follows: % activation = (sample-DMSO control)/DMSO control \times 100. For lead compounds, the minimal compound concentration that enhanced ROS production by 50% above background control cells (AC_{50}) was determined by graphing

the percentage activation of ROS versus the logarithm of concentration of test compound. Each curve was determined using five to seven compound concentrations.

For selected compounds, ROS production was determined for isolated murine and human neutrophils using the protocol described above, and AC_{50} values were calculated. The final concentration of cells in these assays was 5×10^5 cells/ml.

Ca^{2+} Mobilization Assay. Changes in intracellular Ca^{2+} were measured with a FlexStation II scanning fluorometer using a FLIPR 3 Calcium Assay Kit (Molecular Devices, Sunnyvale, CA). In brief, human neutrophils suspended in HBSS containing 10 mM HEPES were loaded with FLIPR Calcium 3 dye following the manufacturer's protocol. After dye loading, Ca^{2+} was added to the cell suspension (2.25 mM final), and 100 μ l of cell suspension were aliquoted into the wells of a flat-bottomed black microtiter plate (2×10^5 cells/well). The compound source plate contained dilutions of test compounds in HBSS. Changes in fluorescence were monitored ($\lambda_{ex} = 485$ nm, $\lambda_{em} = 525$ nm) every 5 s for 240 to 500 s at room temperature after automated addition of compounds to the cells. Maximum change in fluorescence, expressed in arbitrary units over baseline was used to determine agonist response. Curve fitting and calculation of median effective concentration (EC_{50}) value were determined by nonlinear regression analysis of the dose-response curves generated using Prism 4 (GraphPad Software, Inc., San Diego, CA). Evaluation of all selected test compounds for auto-fluorescence ($\lambda_{ex} = 485$ nm; $\lambda_{em} = 525$ nm) indicated they had no background fluorescence in the Ca^{2+} mobilization assay buffer system (data not shown).

For desensitization assays, 5 nM/MLF (EC_{50} dose) was first added to cells, followed by incubation for 4 min and then addition of test compounds or 5 nM fMLF. Reactions were monitored for an additional 4 min.

Chemotaxis Assay. Neutrophil chemotaxis was analyzed in 96-well ChemoTx chemotaxis chambers (Neuroprobe, Gaithersburg, MD). Lower wells were loaded with 30 μ l of HBSS⁺ containing 2% fetal bovine serum and the indicated concentrations of test compound, DMSO (negative control), or 50 nM IL-8 (positive control). Neutrophils suspended in HBSS⁺ containing 2% fetal bovine serum (2×10^6 cells/ml) were added to the upper wells and allowed to migrate through a 5.0- μ m pore polycarbonate membrane filter for 60 min at 37°C and 5% CO_2 . After incubation, the upper wells were gently aspirated from the filter, 2.5 mM EDTA was added to the upper wells for 5 min, and the wells were rinsed again to remove remaining cells. The plates were centrifuged (800g) for 5 min to dislodge any cells adhering to the underside of the filter, and the filter was removed. The number of migrated cells was determined by measuring ATP in lysates of transmigrated cells using a luminescence-based assay (CellTiter-Glo; Promega, Madison, WI). Luminescence measurements were converted to absolute cell numbers by comparison of the values with standard curves created by aliquoting known numbers of neutrophils into the lower wells of a ChemoTx plate and processing then identically to the test sample wells. The results are expressed as percentage of negative control and were calculated as follows: (number of cells migrating in response to test compounds自ontaneous cell migration in response to control medium) \times 100. EC_{50} values were determined by nonlinear regression analysis of the dose-response curves generated using Prism 4 software.

Conformational Analysis. For selected agonists, sets of conformations were generated using the Conformational Search Module, as implemented in HyperChem Version 7.0 (Hypercube, Inc., Waterloo, ON, Canada). The systematic search of conformations for each compound was performed by energy minimization, starting with 1000 to 2000 initial geometries at random values of torsion angles about exocyclic single bonds and chemical bonds within nonaromatic cycles. Energy was minimized by the Polak-Ribiere conjugate gradient method with MM+ force field (HyperChem). Attainment of a root-mean-square gradient <0.02 kcal/mol $\cdot \text{\AA}$ was used as the termination condition for minimization. Conformations were considered

equivalent if all the corresponding torsion angles differed by less than 20° among conformations. Results of the conformational search were saved as text files in HCS format adopted in HyperChem. These files were used as input for a computer program that analyzed each conformation and calculated distances between atoms specified by user as potential acceptors of H-bonds or hydrophobic points. We placed the hydrophobic centers in the middle of aromatic or thiophene rings, whereas the acceptor centers were positioned at hydroxyl, carbonyl, ether, or ester oxygen atoms, which are known as strong H-bond acceptors. The distances calculated were compared with those in the pharmacophore model published previously by Edwards et al. (2005).

Results

High-Throughput Screening for Compounds that Activate the Phagocyte ROS Production. To identify novel compounds that activate functional activity of phagocytes, we screened a library of compounds with molecular masses from 200 to 550 Da. This library was randomly assembled to maximize chemical diversity with commonly accepted pharmaceutical hit substructures, including 6118 compounds containing an amide linker. However, the library did not contain lipids or compounds with metal-organic, aminoglycoside, and macrocyclic scaffolds, all of which have been reported previously as stimulators of neutrophil functions (Kenny et al., 1992; Labro, 2000). The main substructures included in the parent 10,000-compound chemolibrary are summarized in Table 1.

ROS generation was used as an index to monitor phagocyte functional activity after treatment with a test compound. Because test compounds were delivered in DMSO, we first evaluated the effects of DMSO on our assay system and found that 1% DMSO inhibited the luminescence signal produced by PMA-stimulated bone marrow leukocytes in a peroxidase-free detection system ($\sim 70\%$ decrease in signal versus non-DMSO control) (data not shown). Indeed, DMSO is a potent hydroxyl radical scavenger (Klein et al., 1981) and has been reported to suppress ROS production in neutrophils stimulated by different compounds (Beilke et al., 1987). To address this issue, we found that addition of HRP to the assay significantly attenuated the inhibitory effect of 1% DMSO on ROS production by PMA-stimulated bone marrow leukocytes in the luminescence-based assay ($<20\%$ decrease in signal versus non-DMSO control) (data not shown). Thus, this assay system was used for primary screening. Note that addition of HRP has been shown previously to enhance ROS detection in luminol-based assay systems (Lundqvist and Dahlgren, 1996). In addition, baseline luminescence due to ROS production in unstimulated, resting cells was completely inhibited by 10 U/mL superoxide dismutase, demonstrating specificity of this assay system (data not shown).

Using the primary assay system described above (L-012/HRP), we evaluated the effect of each compound on ROS production in bone marrow leukocytes, and a compound was defined as a lead if it exhibited >2 -fold enhancement of ROS production compared with baseline ROS production at a final compound concentration of 20 μ g/ml. Primary screening resulted in the selection of 523 compounds from the parent library (5.2% hit rate) with putative phagocyte activating properties, and further dose-response analyses were per-

formed with these compounds using standard luminescence-based assay conditions with bone marrow leukocytes. As examples, representative kinetic curves and dose-response curves for compounds **1** and **9** are shown in Fig. 1. Notice that individual compounds stimulated ROS production with distinct kinetics, some inducing a bimodal response (Fig. 1A) and others inducing a unimodal response (Fig. 1B). For primary screening, we determined AC_{50} instead of standard EC_{50} values; it was difficult to determine the real effective concentration in many cases because some of the test compounds were insoluble and/or inhibited the cell response at

increasing concentrations of compound. As result of the dose-response analyses, 56 compounds were found to have AC_{50} values $<35 \mu\text{M}$. In general AC_{50} values in the murine neutrophil-based assay were ~ 2 -fold higher than those determined with bone marrow leukocytes (Table 2). However, it should be noted that a good linear correlation was found [$r = 0.727$; $n = 55$; one outlier (compound **3**) was excluded] by plotting the negative logarithm of AC_{50} values for isolated murine neutrophils versus the negative logarithm of AC_{50} values for bone marrow leukocytes (Supplemental Figure S1), indicating that the use of bone marrow leukocytes in

TABLE 1

Comparison of substructures and atoms of compounds in the parent library and active set

Molecular Substructure or Atoms	Number (%) of Compounds in the Sets with Indicated Substructures or Atoms		% Compounds in Active Set/% Compounds in Parent Set
	In Parent Set ($n = 10,000$)	In Active Set ($n = 26$)	
Amide linker	6118 (61.18)	21 (80.8)	1.3
Halogen atoms (Cl, Br, F)	3811 (38.11)	5 (19.2)	0.5
Six-membered <i>N</i> -containing heterocyclic derivatives	1751 (17.5)	2 (7.7)	0.4
Nitrile	1001 (10.01)	0 (0)	0
Five-membered <i>N</i> -containing heterocyclic derivatives	931 (9.31)	7 (26.9)	2.9
Thiophene ring	852 (8.52)	8 (30.8)	3.6
Furan ring	730 (7.30)	4 (15.4)	2.1
Sulfonamide linker	336 (3.36)	0	0
Phenylurea	190 (1.90)	1 (3.8)	2.0
<i>t</i> -Butyl	180 (1.8)	9 (34.6)	19.2
Terminal sulfonamide	100 (1.00)	1 (3.8)	3.8
<i>t</i> -Butyl benzene	42 (0.42)	6 (23.1)	55.0
Thiophene-2-amide-3-carboxylic ester	47 (0.47)	6 (23.1)	49.2
1,3-Benzodioxolane-5-carboxylic amide	31 (0.31)	1 (3.8)	12.3

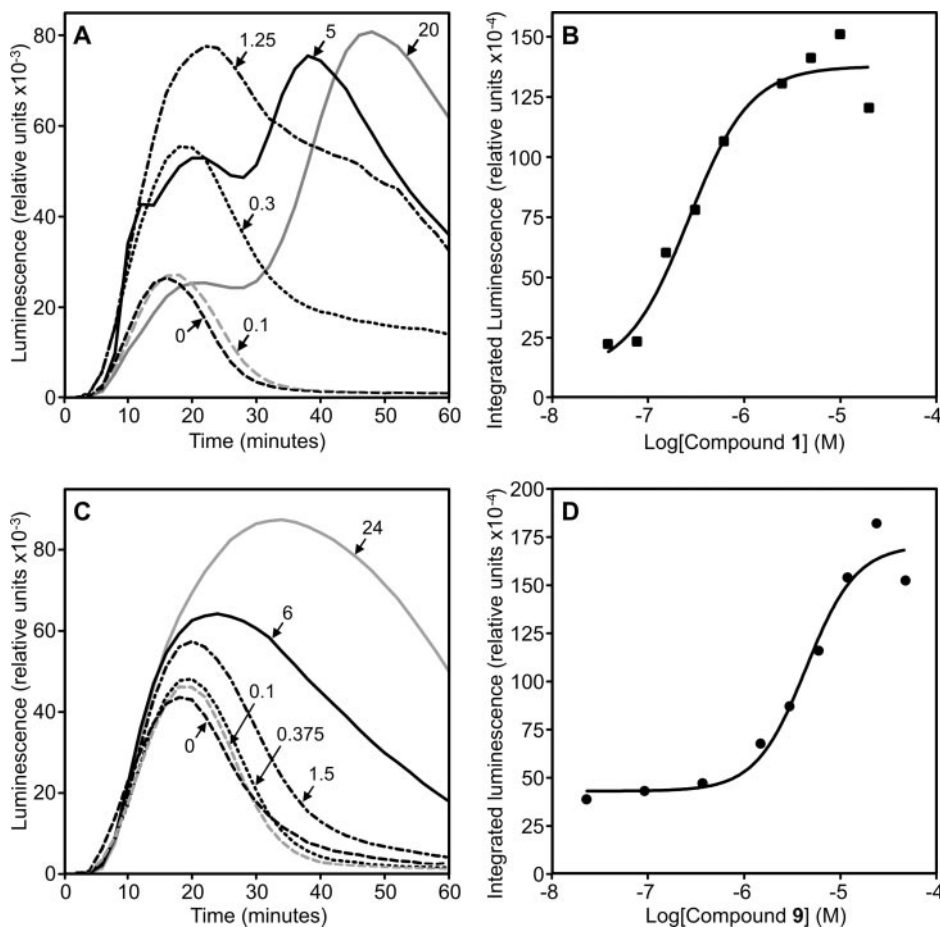


Fig. 1. Representative examples of bone marrow leukocyte activation by test compounds. Bone marrow leukocytes were treated with the indicated concentrations of compound **1** (A and B) and compound **9** (C and D), and ROS production was monitored using an L-012/HRP-amplified assay system. A and C show kinetic curves of ROS production induced by the concentrations of compound (in micromolar) indicated for each curve. B and D show integrated luminescence (1 h) induced in bone marrow leukocytes plotted against the logarithm of compound concentration. A representative experiment from three independent experiments is shown.

TABLE 2

Chemical structures and activity of the most potent activators of ROS production

Compound activation of ROS production is indicated for bone marrow leukocytes (BM), murine neutrophils (M PMN), and human neutrophils (H PMN).

Compound Number & Structure		AC ₅₀			Compound Number & Structure		AC ₅₀		
		BM	PMN				BM	PMN	
			M					H	M
		μM					μM		
1		0.1	0.05	8.31	14		6.2	24.7	38.6
2		1.7	2.0	4.9	15		6.3	1.6	18.4
3		1.9	26.8	N.A.	16		6.6	0.6	N.A.
4		2.3	8.7	2.3	17		6.7	27.0	N.A.
5		2.4	12.2	9.6	18		8.5	5.6	N.A.
6		2.6	1.3	N.A.	19		8.6	12.0	17.3
7		2.7	1.7	N.A.	20		8.9	11.8	N.A.
8		2.8	1.7	N.A.	21		11.3	34.0	N.A.
9		3.4	1.4	4.3	22		12.6	15.1	3.8
10		3.6	15.0	N.A.	23		14.3	3.2	3.2
11		3.6	7.1	7.1	24		15.2	3.8	N.A.
12		3.7	NA	N.A.	25		16.7	1.3	N.A.
13		4.5	4.1	N.A.	26		19.8	12.8	2.0

N.A., cell activation was <50% of control level over a concentration range of 0 to 40 μM .

primary screening provided a reasonable approach for identifying neutrophil agonists.

The size of the hit set was further reduced by applying a series of experimental filters to eliminate insoluble compounds and oxidants/reductants, which could nonspecifically activate cells or react with the ROS assay system components. These filters included microscopic determination of insoluble aggregates and evaluation of ROS-inducing activity of the compounds in bone marrow leukocytes after filtration of the test compounds through a 0.22- μ m filter. In this primary screening, compounds with low water solubility were filtered out because crystals of substances are known to activate neutrophils (Jackson et al., 2000). Compounds that directly induced luminescence or reduced cytochrome *c* in the absence of cells were also filtered out (Nemeikaite-Ceniene et al., 2005). Interestingly, 13 nitrile derivatives with relatively high neutrophil-activating properties were present in the group of compounds removed by these filters. Based on the results of these filters, we selected 26 compounds with the highest activity ($AC_{50} < 20 \mu$ M) as a set of prospective agonists for analysis in human neutrophils. Structures of the selected compounds and their activities are presented in Table 2.

Effect of the Hit Compounds on Human Neutrophils Functional Responses. Hit compounds identified in murine neutrophil screening were evaluated for their ability to activate human neutrophil ROS production, and we found that 12 of the 26 lead compounds activated human neutrophil ROS production with AC_{50} values in the range of 1.9 to 38.6 μ M (Table 2). To further investigate the effects of test compounds on human neutrophil function, we evaluated the ability of these compounds to induce Ca^{2+} mobilization and chemotaxis. First, we tested the 56 compounds identified by primary screening and found six compounds that dose dependently activated intercellular Ca^{2+} ($[Ca^{2+}]_i$) release in human neutrophils with EC_{50} values $< 25 \mu$ M (Table 3 and Fig. 2). Note that five of these compounds were present in the 26-compound active set (Table 2). Compounds **1**, **2**, **22**, and **30** induced $[Ca^{2+}]_i$ release at low micromolar concentrations, whereas compounds **14** and **26** activated Ca^{2+} release at

nanomolar concentrations (Table 3). In addition, effects of compounds on the $[Ca^{2+}]_i$ response were consistently observed between different donors. As shown in Fig. 2, kinetics of the $[Ca^{2+}]_i$ response differed between compounds. For example, addition of either control fMLF or compounds **14**, **26**, and **30** caused a rapid increase in $[Ca^{2+}]_i$ that peaked by 1 min and gradually declined to basal values, reflecting clearance of Ca^{2+} from the cytosol (Fig. 2A). In contrast, $[Ca^{2+}]_i$ increased after a lag of ~ 1 min after compound **22** treatment and remained elevated for at least 5 min after treatment (Fig. 2A). Likewise, a lag of ~ 1 min was observed after treatment with compounds **1** and **2**; however, maximal levels of $[Ca^{2+}]_i$ were not achieved until ~ 10 min after treatment and these levels were sustained for at least 20 min (Fig. 2B). The sustained level of $[Ca^{2+}]_i$ induced by compounds **1**, **2**, and **22** suggests that these compounds may use distinct pathways for neutrophil activation that are different from those used by fMLF. To determine the origin of the $[Ca^{2+}]_i$ elevation caused by the selected compounds, human neutrophils were stimulated with test compounds in the absence of extracellular Ca^{2+} in the medium. All six compounds still evoked $[Ca^{2+}]_i$ responses in the absence of extracellular Ca^{2+} , although the levels of $[Ca^{2+}]_i$ achieved were much lower than those observed in the presence of extracellular

TABLE 3

Effect of selected test compounds on Ca^{2+} mobilization and chemotaxis in human neutrophils

Compound Number	EC_{50}	
	Ca^{2+} Mobilization	Chemotaxis
	μ M	
1	6.18 ± 0.13	NA
2	5.08 ± 1.76	0.56 ± 0.38
14	0.63 ± 0.39	0.042 ± 0.002
22	23.64 ± 2.99	9.57 ± 1.13
26	0.73 ± 0.22	12.55 ± 5.08
30 ^a	14.23 ± 1.45	10.90 ± 2.39
104	12.20 ± 4.35	3.45 ± 0.20
fMLF	0.005 ± 0.001	0.0005 ± 0.0001

^a Structure of compound 30:

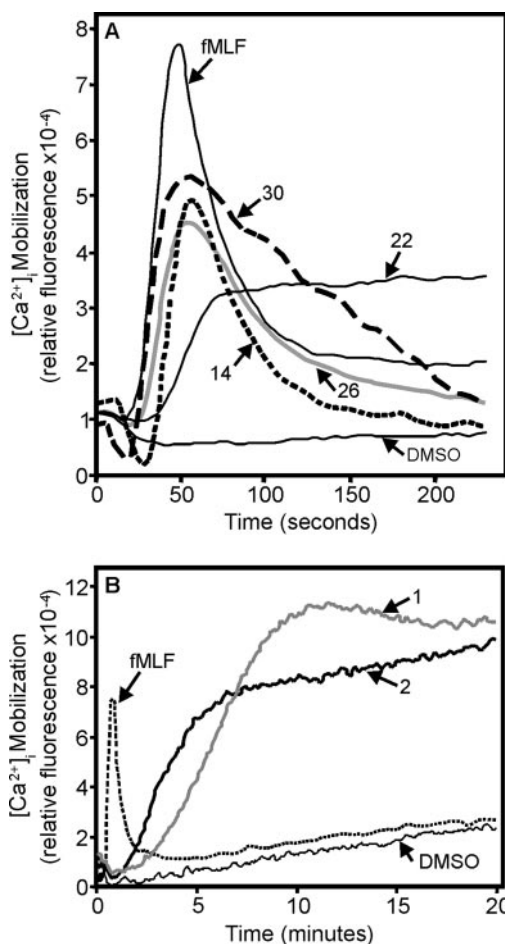
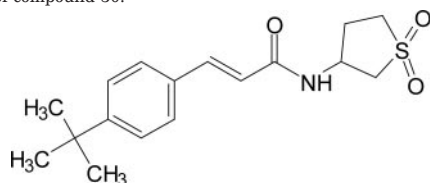


Fig. 2. Representative kinetics of Ca^{2+} mobilization after treatment with lead compounds. Human neutrophils were treated with the indicated test compounds (EC_{50} dose), 5 nM fMLF (positive control), or 1% DMSO (negative control), and $[Ca^{2+}]_i$ flux was monitored for the indicated times. The results shown are representative of three independent experiments from different blood donors.

Ca^{2+} (data not shown). Thus, these results indicate that the selected compounds can induce release of intracellular Ca^{2+} stores but that most of the $[\text{Ca}^{2+}]_i$ response resulted from extracellular Ca^{2+} influx.

Five compounds (**2**, **14**, **22**, **26**, and **30**) were found to be neutrophil chemoattractants and dose-dependently induced neutrophil migration with EC_{50} values of 40 nM to 13 μM (Table 3), and a representative dose-response curve is shown in Supplemental Figure S2. Thus, except for the thiophene derivative (compound **1**), the selected compounds that activated Ca^{2+} mobilization were also chemoattractants.

Because compound **14** was a potent activator of neutrophil Ca^{2+} mobilization and chemotaxis, we searched the parent library of other analogs bearing the 1,3-benzodioxolane-5-carboxylic acid benzylidene-hydrazide scaffold. This substructure was selected from the molecule because it contained all three pharmacophore points characteristic of FPR

ligands (see *Conformational Analysis*). The parent compound library contained six such analogs (Table 4). Analysis of these analogs showed that compound **104** was a potent neutrophil agonist, inducing Ca^{2+} mobilization and chemotaxis (Table 3). Indeed, the kinetics of Ca^{2+} mobilization induced by compound **104** were also quite similar to those of fMLF (data not shown). The other five analogs had lower activity, inducing $[\text{Ca}^{2+}]_i$ responses considerably lower than 5 nM fMLF (Table 4). One reason for the lower activity of these compounds may be that they contain a carbonyl group in substituent R, which could lead to the formation of intermolecular H-bonds and attenuate interaction of these compounds (**105-109**) with an appropriate receptor.

The response patterns observed for our hit compounds listed in Table 4 suggested they could be agonists of G protein-coupled receptors (GPCR), as is the case for many neutrophil chemoattractants (Zhelev and Alteraifi, 2002). To

TABLE 4

Effect of 1,3-benzodioxolane-5-carboxylic acid benzylidene-hydrazide derivatives on neutrophil Ca^{2+} mobilization
fMLF response is the maximal $[\text{Ca}^{2+}]_i$ mobilization expressed as a percentage of response induced by 5 nM fMLF

Compound Number	R	EC_{50}	fMLF Response
		μM	%
14		0.63 ± 0.39	90
104		12.2 ± 4.35	75
105		N.A.	<15
106		N.A.	<15
107		N.A.	<15
108		N.A.	<10
109		N.A.	<5

N.A., very low response/non-active compound.

evaluate this hypothesis, we tested the effect of pertussis toxin (PTX), a specific inhibitor of G_i/G_o -proteins, on Ca^{2+} mobilization in human neutrophils stimulated by the compounds listed in Table 3. As shown in Fig. 3, PTX (2 μ g/ml) blocked $[Ca^{2+}]_i$ influx in human neutrophils treated with control f MLF (0.6–100 nM) or with compounds **1**, **2**, **14**, **26**, **30**, and **104**, whereas PTX treatment had no significant effect on the $[Ca^{2+}]_i$ flux induced by compound **22**. The results indicate that at least six of our lead compounds are likely to activate human neutrophils through PTX-sensitive GPCR(s). Note, however, that the slopes of the dose-response curves and effects of PTX varied among compounds, suggesting differences in affinity and/or binding target. In addition, the highest concentrations of test compounds may cause nonspecific effects, because the data do not fit as well to the dose-response curves for high concentrations of some compounds.

Human neutrophils express FPR/FPRL1, which is a remarkably promiscuous receptor (Nanamori et al., 2004; Edwards et al., 2005). Therefore, we considered the possibility that some of the test compounds were ligands for FPR/FPRL1 by testing the effect of Boc-2, a specific antagonist of FPR/FPRL1 (Gavins et al., 2003). As shown in Fig. 3, pretreatment of human neutrophils with 10 μ M Boc-2 strongly inhibited Ca^{2+} mobilization in neutrophils stimulated with control f MLF or compounds **14**, **30**, and **104**. By comparison, Boc-2 failed to inhibit Ca^{2+} mobilization induced by compounds **22** and **26** and even enhanced the $[Ca^{2+}]_i$ response induced by compounds **1** and **2**. Overall, these results suggested that compounds **14**, **30**, and **104** might be novel agonists for FPR/FPRL1. To further evaluate this issue, we examined whether f MLF pretreatment desensitized the neutrophil response to compounds **14**, **30**, and **104**. After 5 min pretreatment with 5 nM f MLF, the cells were treated with f MLF or the selected compounds at an EC_{100} dose. As demonstrated in Fig. 4 (f MLF pretreatment, dashed curves; vehicle pretreatment, solid curves), pretreatment with 5 nM f MLF markedly attenuated Ca^{2+} mobilization induced by control f MLF (homologous desensitization) as well as by compounds **14**, **26**, **30**, and **104**. Furthermore, when the neutrophils were pretreated with 50 nM f MLF, they could not respond at all to compound **14** (data not shown). In comparison, f MLF pretreatment had no effect or even enhanced Ca^{2+} mobilization induced by compounds **1**, **2**, and **22** (Fig. 4, dashed lines), which is similar to the enhancement observed when Boc-2-treated cells were activated with compounds **1** or **2** (Fig. 3, B and C).

Substructure Analysis and Fragment Focusing. Examination of the structures representing the most potent phagocyte agonists (Table 2) revealed that these compounds contained at least two hydrophobic centers separated by a 3–10 chemical bond-linker and at least 2 to 3 potential acceptors for H-bonding (carbonyl, ester, ether, or hydroxyl oxygen atoms). Half of the 26 compounds contained two main classes of molecular fragments, and compounds containing either a *t*-butyl benzene fragment or a thiophene-2-amide-3-carboxylic ester substructure were enriched ~50-fold compared with their relative representation in the parent set (Table 1). In contrast, the relative proportion of compounds containing amide and sulfonamide linkers, 5/6-membered *N*-containing heterocycles, furans, phenylureas, or halogen atoms was not substantially different between parent and active sets of compounds.

To determine essential molecular scaffolds associated with neutrophil-activating properties, we conducted a comparison of the main chemical substructures among the 26 selected neutrophil activators with a number of previously published activators of phagocytes and/or neutrophil receptor agonists (see Supplemental Table S1). Most of these compounds are either direct activators or priming agents of neutrophils; however, lipids, phorbol ester derivatives, and aminoglycoside and macrocyclic antibiotics were not included here because they contain structural scaffolds that were not present in our parent chemolibrary. The main scaffolds present in reported phagocyte agonists and their distributions in our parent library are shown in Table 5. Although there was no general scaffold present in all previously reported structures, most of these compounds contain at least one benzene ring or heterocycle and/or iso-*t*-butyl group (Table 5). Three compounds (enalaprilat, pidotimod, and Pro-Pro) contain the substructure designated as scaffold II and are Pro-related compounds. In addition, indomethacin, MK-886, tiprotimod, tuftsin, anisomycin, and a C5a agonist contain a similar scaffold with a carboxyl-containing aliphatic group located at various positions of a five-membered heterocycle (data not shown). Thus, 10 of 30 reported phagocyte activators contain scaffold II or a related substructure. It should also be noted that 6 of the 26 most potent agonists identified here (compounds **1**, **6–8**, **15**, and **16**) (hit rate 23.1%) contain scaffold II expressed as a thiophene-amide ester substructure (Tables 1 and 2). In general, scaffold II may be similar to damage-associated Pro-related molecular patterns, although the targets involved in their recognition have yet to be identified.

Previously reported phagocyte agonists also contained other substructures that were present in the parent library. It is noteworthy that amorolfine contains a *t*-butyl benzene scaffold, which is characteristic of our most potent neutrophil agonists (compounds **2**, **19**, **20**, **21**, **23**, and **25**). Terbutaline, terbutaline, and MK-886 also contain the *t*-butyl group. However, most other substructures found in previously reported neutrophil activators, except for compounds **9** and **25**, were not present in the highly active prospective set because these compounds had AC_{50} values > 20 μ M (Table 5).

Based on substructure analysis and analysis of structures for previously reported phagocyte agonists, two series of compounds (*t*-butyl benzene derivatives and thiophene-2-amide-3-carboxylic esters) were extracted from the parent chemical diversity set for further SAR analyses. The parent library contained 42 *t*-butyl benzene derivatives, and 16 of these were agonists of murine neutrophils (AC_{50} < 40 μ M; hit rate 38.1%), whereas six were potent agonists of human neutrophils (AC_{50} < 20 μ M) (Supplemental Table S2). Forty-seven thiophene-2-amide-3-carboxylic esters were present in the parent library, although many of these compounds were not selected in primary screening because of their lower solubility. Rescreening of these derivatives (Supplemental Table S3) showed 27 were activators of ROS production in bone marrow leukocytes (AC_{50} < 20 μ M; hit rate of 57.5%). Of these compounds, 16 were potent activators of isolated murine neutrophils (AC_{50} < 4 μ M; hit rate 34.0%), but only two (**1** and **15**) activated human neutrophils. Therefore, it seems that the thiophene derivatives are more specific for murine neutrophils versus human neutrophils.

Conformational Analysis. Recently, Edwards et al. (2005) developed a pharmacophore model for FPR ligands

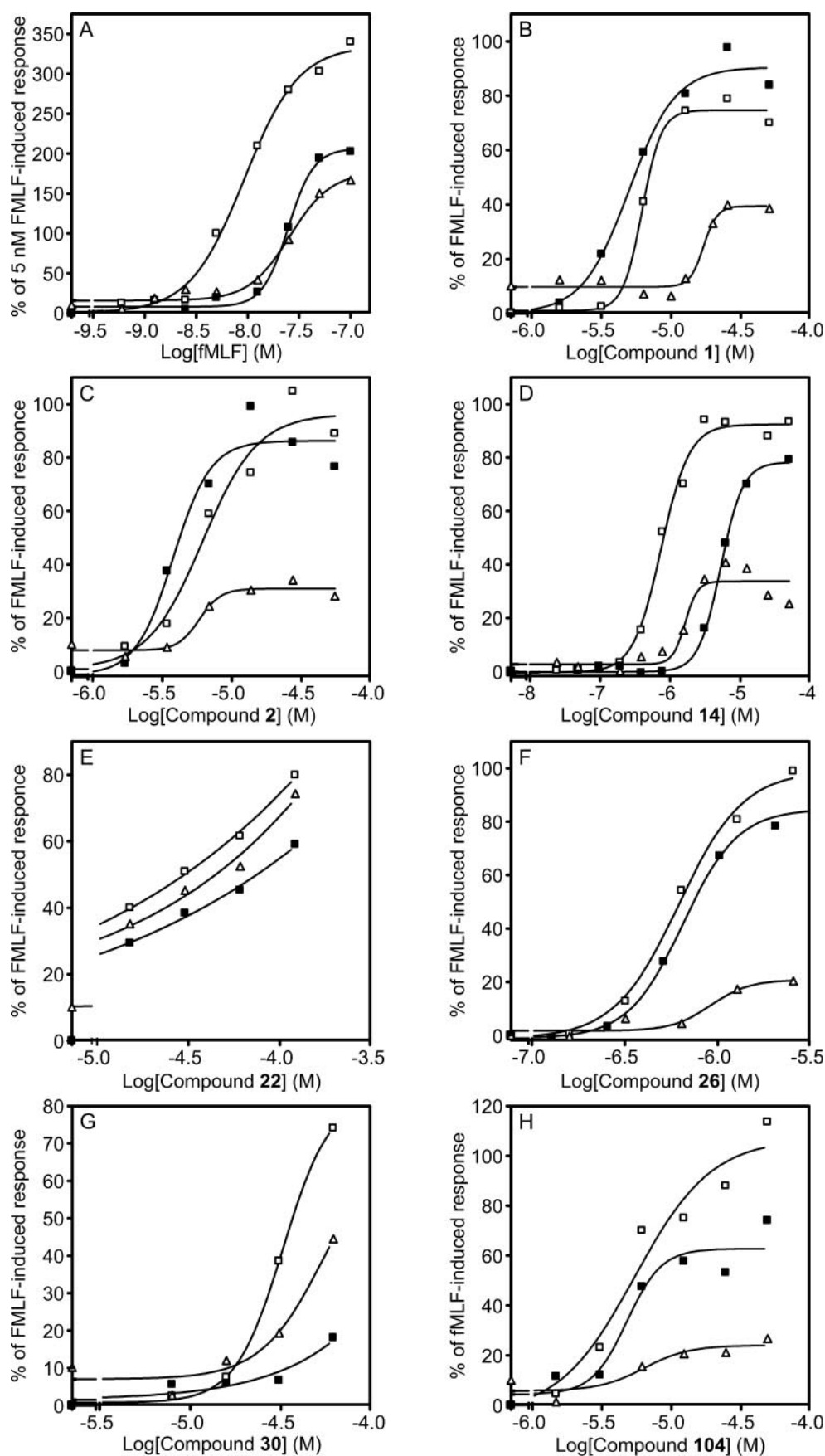


Fig. 3. Effect of PTX and Boc-2 on Ca^{2+} mobilization in human neutrophils stimulated with fMLF or the indicated test compounds. Neutrophils were incubated with FLIPR Calcium 3 dye and PTX (\triangle), Boc-2 (\blacksquare), or without inhibitor/antagonist (\square) for 30 min before analysis of $[\text{Ca}^{2+}]_i$ flux, as described. Responses were normalized to the response induced by 5 nM fMLF, which was assigned a value of 100%. Values represent the average means of triplicate measurements. The data presented are from experiments taken from a minimum of three independent experiments using different blood donors.

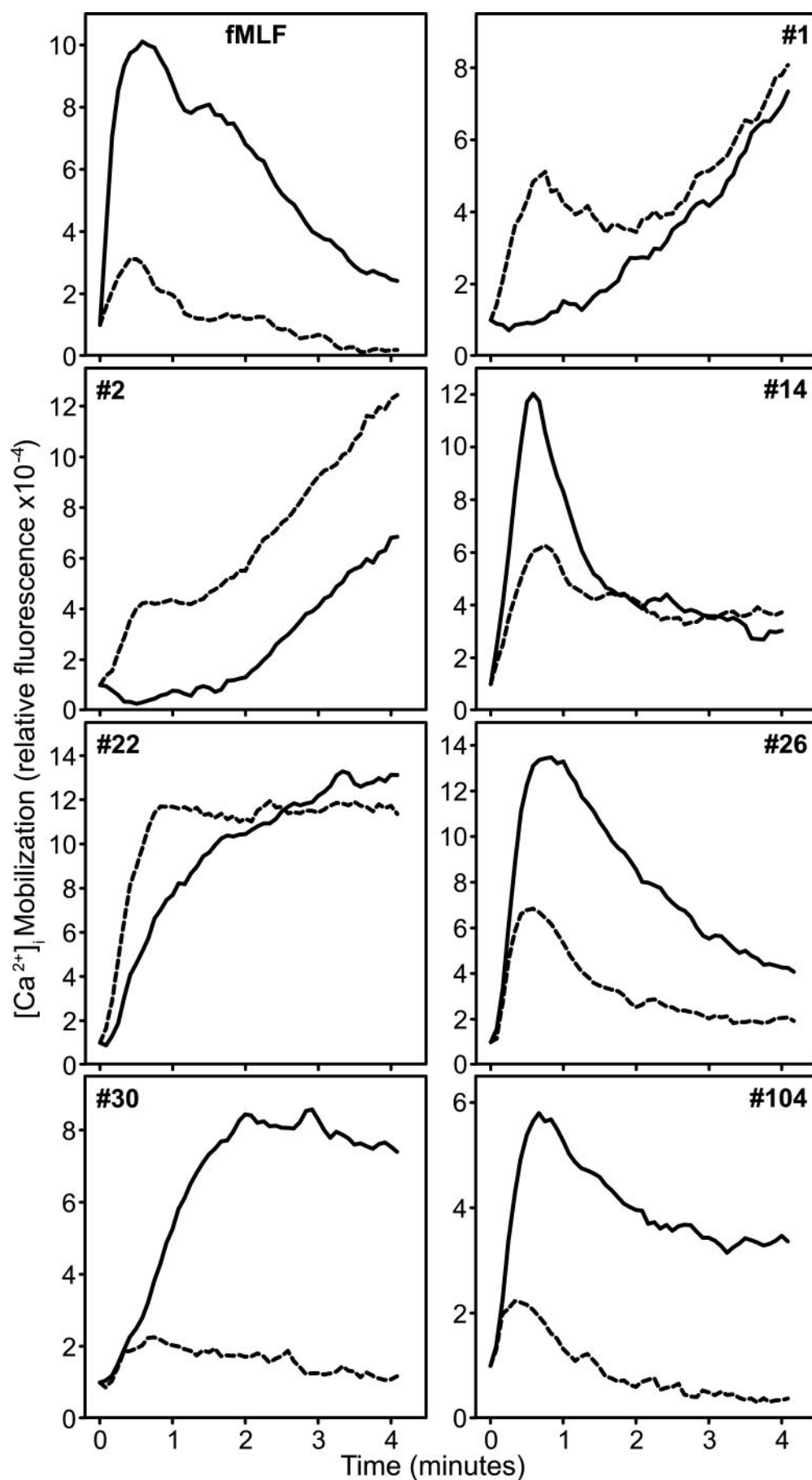


Fig. 4. Effect of fMLF pretreatment on Ca^{2+} mobilization induced by selected test compounds. Human neutrophils were loaded with FLIPR Calcium 3 dye and pretreated with 5 nM fMLF (dashed curves) or vehicle (solid curves) for 5 min, followed by a second addition of 5 nM fMLF or addition of the indicated test compound (EC_{100} dose) (second addition occurred at time 0 on the graph). Ca^{2+} mobilization was monitored, as described, and the data are presented as relative fluorescence intensity. Data from a representative experiment are shown from a minimum of three independent experiments using different blood donors.

that was based on results of docking of known receptor agonists and antagonists onto a homology model of the receptor. This model has three points: two acceptors for H-bonding and one hydrophobic point. Using this pharmacophore model, we evaluated distances between the pharmacophore points for low-energy conformations of the seven small-molecule neutrophil agonists shown in Table 3. To verify that the model was more specific for FPR versus FPRL1, appropriate dis-

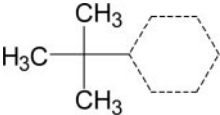
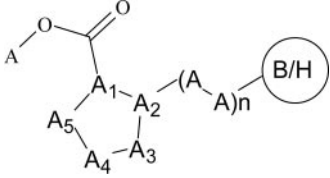
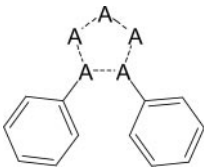
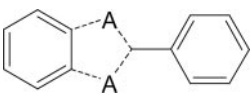
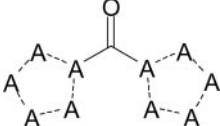
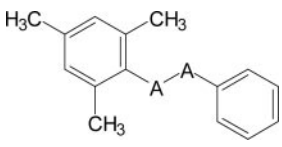
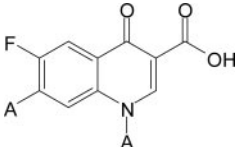
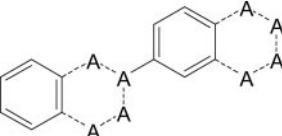
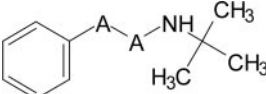
tances in conformations of a small-molecule agonist of FPRL1, Quin-C1 (Nanamori et al., 2004), were also estimated.

Although our neutrophil activators represent a diverse set of compounds, visual inspection of their structures allowed us to identify two acceptors for H-bonding and at least one hydrophobic site in six of the seven selected compounds. Compound **2** was not analyzed because it did not contain two

TABLE 5

Scaffolds present in previously-reported neutrophil agonists and their representation in the active set (N_1) and parent library (N_2)

Active set = 26 compounds and parent library = 10,000 compounds. Dashed lines in the structures represent any bond type, and A represents any atom except H. Compounds were considered active if $AC_{50} < 20 \mu\text{M}$ in the bone marrow leukocyte-based assay. In scaffold II, B/H represents a benzene ring or 5-membered heterocycle.

Scaffold	Name of Agonist	Reported Substructure of Agonist	N_1/N_2	Hit Agonist
I	Amorolfine		8/77	Compounds 2 , 4 , 16 , 19 , 20 , 21 , 23 , 25
II	Enalaprilat, Pidotimod, Pro-Pro		6/63	Compounds 1 , 6 , 7 , 8 , 15 , 16
III	Celecoxib		1/49	Compound 25
IV	Benoxaprofen		0/43	
V	Pidotimod, Pro-Pro		0/28	
VI	m-3M3FBS		0/7	
VII	Grepafloxacin, Norfloxacin		0/5	
VIII	Kazinol B		0/3	
IX	Terbutaline		1/2	Compound 9

appropriate acceptors for H-bonding. Considering that these are flexible molecules, we explored their potential energy surfaces using a conformational search with an MM+ force field, and the conformations within an energy gap of 6 kcal/mol over the global minimum (Nicklaus et al., 1995) were stored. The numbers of nonequivalent conformations (N_{conf}) found for each of the compounds investigated are shown in Table 6, and calculated distances that fit model tolerances are indicated in bold. N_{conf} values differed significantly, depending on the flexibility of the compounds. The most active agonist (compound **14**) had 710 conformations, and three of these conformations fit quite well into the pharmacophore model, meeting appropriate tolerance distances (Table 6 and Fig. 5). The less active compounds **22**, **30**, and **104** had arrays of 788, 48, and 379 N_{conf} , respectively, and two of these conformations fit well into the pharmacophore model for each compound (Table 6). Although compound **22** has two conformations with good fit, the long acyl tail at the benzene ring may result in an unfavorable steric interaction in the area of the putative receptor. One fitted conformation was found for compound **1**; however, this conformation had a 5.0 Å-distance for A_1 -H, which is on the low range of tolerance for this distance. Conformations for both compound **26** and Quin-C1 did not fit well into the model, as one of three distances between their pharmacophore points were out of tolerance distances for their best-fit conformations (Table 6).

Discussion

The identification of agents that enhance innate immune responses represent a promising approach for increasing host resistance to infection (Schiller et al., 2006). In the present report, we used high-throughput screening of a large chemical diversity library to identify unique small-molecule activators of neutrophils. For primary screening, we used murine total bone marrow leukocytes, because various neutrophil purification techniques have been shown to alter cell responsiveness, either activating or impairing cellular responses (Zahler et al., 1997). Thus, the use of unpurified leukocytes

minimizes phagocyte activation during isolation and thus more accurately reflects the physical condition of these cells in vivo. This is a reasonable approach for primary screening of phagocyte agonists, in that ROS generation in bone marrow preparations is due primarily to neutrophils and macrophages, and lymphocytes present do not release detectable ROS (Li and Chung, 2003). After primary screening and filtering of compounds, we then moved to analysis of effects on purified murine neutrophils, followed by final confirmation with human neutrophils. It is noteworthy that screening with murine neutrophils resulted in the identification of 26 compounds that activated ROS production; however, only 12 of these compounds were effective activators of human neutrophils. Thus, these data provide further indication of differences in responsiveness between human and murine phagocytes, and further analysis of compounds that selectively activate murine neutrophils may provide clues to explain such species-specific differences in responsiveness.

It is interesting that luminescence responses induced by test compounds varied between individual compounds, resulting in either unimodal or bimodal curves (see Fig. 2). Because the various agonists identified here were found to use different pathways, including FPR and non-FPR pathways, it is reasonable that distinct response patterns would be induced. Such variations in luminescence responses have been reported previously and have been suggested to be related to differential effects of agonists on degranulation, Ca^{2+} flux, phospholipase D, and/or protein kinases in the cell (Arnhold et al., 1999; Nemeth et al., 2002; Daiber et al., 2004; Petkovic et al., 2005). For example, a bimodal luminescence

TABLE 6

Number of representative conformations found for test compounds and distances between pharmacophore centers in the low-energy conformations best fit to the published pharmacophore model of FPR ligands. Compound 2 was not fit to the model because it lacked two appropriate acceptors for H-bonding. N_{conf} is the number of representative conformations within 6 kcal/mol of the global minimum. Permitted intervals between pharmacophore points (A_1 and A_2 = hydrogen bond acceptors; H = hydrophobic center) of FPR ligands are indicated in parentheses (Edwards et al., 2005). Distances that do not fit model tolerances are indicated in bold.

Compound	N_{conf}	Distances in the Best-Fit Conformations		
		A_1 - A_2 (3–6 Å)	A_1 -H (5–7 Å)	A_2 -H (4–7 Å)
		Å		
1	78	4.5	5.0	4.3
2	103			
14	710	5.1	6.6	4.9
		5.9	6.3	5.5
		5.8	6.8	5.9
22	788	3.6	6.1	5.5
		3.6	5.7	5.8
26	352	5.1	5.9	3.8
30	48	6.2	5.9	4.7
		5.9	6.2	4.7
104	379	5.9	6.3	5.6
		5.8	6.8	6.0
Quin-C1	906	5.1	7.6	5.9

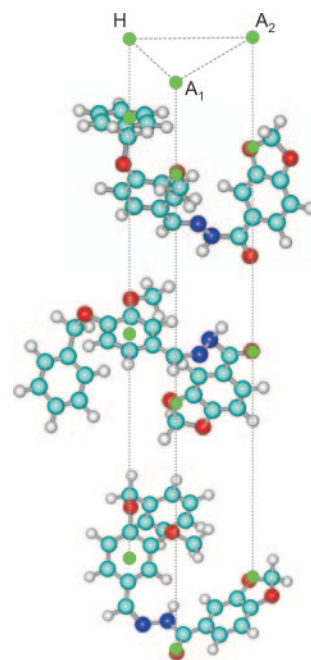


Fig. 5. Comparison of best-fit conformations of compound **14** with the published pharmacophore model of FPR ligands. The three conformations shown for compound **14** represent the best root-mean-square fit from all energy minima within 6 kcal/mol of the global minimum. The conformations are shown in one projection, and the green ellipses are located at their pharmacophore centers. The centers are also indicated at the top of the figure for clarity, with letter notations corresponding to the H-bond acceptors (A_1 and A_2) and hydrophobic center (H), as previously reported by Edwards et al. (2005). For all structures, carbon is sky-blue, nitrogen is blue, oxygen is red, and hydrogen is white.

response has been observed in *f*MLF-treated neutrophils by a number of groups (e.g., see Zalavary and Bengtsson, 1998; Arnhold et al., 1999; Nemeth et al., 2002; Petkovic et al., 2005). Zalavary and Bengtsson (1998) proposed that the initial phase of the *f*MLF-induced oxidative burst was due almost exclusively to extracellular ROS production, whereas the delayed latter phase was due predominantly to intracellular ROS production. On the other hand, Nemeth et al. (2002) proposed that the second phase of ROS production was due to release of myeloperoxidase by activated cells. This mechanism is probably not involved here, however, because HRP was present in the assay media. Arnhold et al. (1999) reported that the first phase of ROS production in *f*MLF-stimulated neutrophils was inhibited by phosphatase inhibitors and was dependent on protein kinase C and phospholipase D activities, whereas the second phase was not dependent on protein kinase C activity. Thus, several mechanisms seem to contribute to variations in luminescence responses observed in activated neutrophils, leading to agonist-specific responses.

In previous searches for neutrophil agonists, high-throughput screening was used to identify several agonists, including a phospholipase C activator (2,4,6-trimethyl-*N*-(*meta*-3-trifluoromethyl-phenyl)-benzenesulfonamide) (Bae et al., 2003) and agonists of C5a, C3a, and FPRL1 receptors (Nanamori et al., 2004; Buck and Wells, 2005; Edwards et al., 2005; Mathieu et al., 2005). Likewise, compounds with phagocyte-activating properties have been identified through analysis of the immunomodulatory side effects of current drugs (Supplemental Table S1). Although many of these reported neutrophil-activating compounds have at least two acceptors for H-bonding, most of them are unrelated to our set of active compounds. Indeed, substructure analysis of previously published phagocyte activators revealed that the compounds identified here represent completely new structural classes of neutrophil agonists.

A number of our lead compounds were highly active, making them promising candidates for further evaluation of immunomodulatory activity in vitro and eventually in vivo. Seven of these compounds were activators of Ca^{2+} mobilization, and six were chemoattractants. Structural analysis of the hit compounds revealed that most of these compounds contained either a *t*-butyl benzene fragment or a thiophene-2-amide-3-carboxylic ester substructure. Among the active *t*-butyl benzene derivatives, a linker chain was present between the *t*-butyl benzene group and a second moiety, R, that was preferentially a benzene ring and/or heterocycle (Supplemental Table S2). In all compounds with high activity (compounds **2**, **19–21**, and **23**) the length of the linker was from five to seven chemical bonds, and a linker of $-\text{C}(=\text{O})-\text{NH}-\text{N}=\text{C}-$ was present in most biologically active *t*-butyl derivatives. Thus, this carboxylic acid hydrazide linker may result in a specific distribution of electron density in the compound. In addition, the nature and size of heterocycle may also determine charge distribution. For example, SAR analysis using general features of the molecules showed that the biologically active compounds have a dumbbell-shaped form, with two bulky moieties connected by a linker of optimal length and nature. This observation suggests that the potential structure of a target molecule in phagocytes would contain two sites at with a distance of ~ 6 to 8 Å. Complementarity of a compound to this putative pseudo-receptor

might then be directed by geometric peculiarities of the ligand; however, charge distribution also seems to be important, because six of seven nonfunctionalized carboxylic acid analogs were inactive. Thus, compound charge/hydrophobicity may be necessary for interaction with its pseudo-receptor.

Among the thiophene derivatives, major differences in structure were due to R_1 – R_3 substituents (Supplemental Table S3). The most potent derivatives ($\text{AC}_{50} < 1$ μM in bone marrow leukocytes) had a cycloheptane (**1** and **98**) or cyclohexane (**88**) group fused to the thiophene ring. Thus, it is possible that these cyclic groups facilitate the appropriate a distribution of hydrophobic zone in the region of the thiophene ring. Although R_3 is a heterocycle in most of the active thiophene derivatives, other substituents are possible, because active compounds **65** and **67** contain CH_3 and CH_2CH_3 at R_3 , respectively. Thus, the primary pharmacophoric points in the thiophene derivatives are probably located inside the thiophene-2-amide-3-carboxylic ester scaffold, which includes 2 acceptors for H-bonding (carbonyl and ester oxygen) and one hydrophobic site in the thiophene ring. It is interesting to note that such a thiophene scaffold was proposed previously for development of anti-inflammatory drugs (Pillai et al., 2005). Furthermore, four compounds with a thiophene-2-amide-3-carboxylic ester scaffold were reported previously as FPR antagonists among 30 other receptor ligands (agonists and antagonists) selected by high-throughput screening, and these derivatives fit well into a three-point pharmacophore model of FPR agonists (Edwards et al., 2005).

Many neutrophil chemoattractant receptors are GPCRs, and GPCR ligation in neutrophils leads to subsequent activation of various cellular responses, including ROS production and Ca^{2+} mobilization (Zhelev and Alteraifi, 2002). Based on the characteristics of our lead compounds, we considered the possibility that some of these compounds also used similar receptor systems. Indeed, several synthetic compounds have been found previously to bind to GPCR and activate neutrophils (Bokoch, 1995; Edwards et al., 2005). Evaluation of the effects of PTX, a specific inhibitor of G_i/G_o -proteins, on neutrophil responses to test compounds indicated that six of the seven lead compounds used PTX-sensitive pathways. Furthermore, we found that the response to one of these compounds (compound **14**) was inhibited by Boc-2, a specific antagonist of FPR/FPRL1. Based on these analyses, as well as pharmacophore modeling, we conclude that compounds **14** and **104** are novel small-molecule agonists of *N*-formyl peptide receptors. Pharmacophore modeling is based on the premise that all ligands of a given target bind in a conformation that presents similar steric and electrostatic features to the target receptor, and these features are recognized by the receptor and are responsible for biological activity (Guner et al., 2004). The pharmacophore model used here was developed based on the bovine rhodopsin crystal structure and known FPR ligands (Edwards et al., 2005). Our molecular modeling showed that compound **14** and its analog, compound **104**, fit quite well with this previously published pharmacophore model, demonstrating a good agreement between biological activity and the presence of low-energy, best-fit conformations of the compounds with the model. Overall, pharmacophore modeling provided further support that these compounds do indeed fit the molecular features required for FPR agonists.

It is noteworthy that the most potent activators of ROS production in murine and human neutrophils (compounds **1**, **2**, and

26) were not FPR agonist, but were still sensitive to PTX treatment. Thus, neutrophil activation by these compounds, as well as compound 1-related analogs, seems to be mediated through GPCRs unrelated to FPR/FPRL1 or possibly could be due to direct G protein activation; however, further characterization will be required to determine their targets and/or mechanisms of action. It is noteworthy that the response to compound 26 was desensitized by fMLF and blocked by PTX; however, it was not blocked by Boc-2. These data suggest that the receptor for compound 26 may be susceptible to cross-desensitization by fMLF. Peptide chemoattractants are well known to regulate leukocyte responsiveness by cross-desensitization of other chemoattractant receptors in a process known as receptor class desensitization, and fMLF can desensitize receptors for C5a and IL-8 (Tomhave et al., 1994), and it is possible that compound 26 binds to one of these receptors. Indeed, the general structure of compound 26 (*N*-[2-(4-methoxyphenyl)ethyl]-*N'*-(4-chlorophenyl)urea) is similar to that of known CXC chemokine receptor 2 (CXCR2) antagonists [*N,N'*-diarylureas such as *N*-(3-bromo-4-cyano-2-hydroxyphenyl)-*N'*-(2-bromophenyl)urea] (Widdowson et al., 2004). Thus, it is conceivable that compound 26 could bind to CXCR2 and that the composition/location of phenyl ring substituents and/or ethylene spacer between the phenyl ring and urea group of compound 26 confers agonist rather than antagonist properties. In support of this idea, removal or replacement of the 2-bromo substituent in nonphenolic ring of the *N,N'*-diarylurea antagonist mentioned above resulted in a significant loss in antagonist activity (Widdowson et al., 2004). Nevertheless, further studies will be needed to investigate this issue. It should be noted that we also identified seven compounds (4, 5, 9, 11, 15, 19, and 23), which stimulated ROS production but did not mobilize $[Ca^{2+}]_i$ in human neutrophils. Whether these compounds activate ROS production independently of Ca^{2+} mobilization or induce subtle effects on $[Ca^{2+}]_i$ flux that are out of the sensitivity range of our assay will need to be determined. Because Ca^{2+} mobilization is not absolutely required for neutrophil ROS production (Geiszt et al., 1999), it is plausible that these compounds could use Ca^{2+} -independent pathways.

References

- Arnhold J, Benard S, Kilian U, Reichl S, Schiller J, and Arnold K (1999) Modulation of luminol chemiluminescence of fMet-Leu-Phe-stimulated neutrophils by affecting dephosphorylation and the metabolism of phosphatidic acid. *Luminescence* 14:129–137.
- Bae YS, Lee TG, Park JC, Hur JH, Kim Y, Heo K, Kwak JY, Suh PG, and Ryu SH (2003) Identification of a compound that directly stimulates phospholipase C activity. *Mol Pharmacol* 63:1043–1050.
- Beilke MA, Collins-Lech C, and Sohnle PG (1987) Effects of dimethyl sulfoxide on the oxidative function of human neutrophils. *J Lab Clin Med* 110:91–96.
- Beutler B (2004) Innate immunity: an overview. *Mol Immunol* 40:845–859.
- Beutler B, Hoebe K, Du X, and Ulevitch RJ (2003) How we detect microbes and respond to them: the toll-like receptors and their transducers. *J Leukoc Biol* 74:479–485.
- Bokoch GM (1995) Regulation of the phagocyte respiratory burst by small GTP-binding proteins. *Trends Cell Biol* 5:109–113.
- Buck E and Wells JA (2005) Disulfide trapping to localize small-molecule agonists and antagonists for a G protein-coupled receptor. *Proc Natl Acad Sci USA* 102:2719–2724.
- Daiber A, August M, Baldus S, Wendt M, Oelze M, Sydow K, Kleschyov AL, and Munzel T (2004) Measurement of NAD(P)H oxidase-derived superoxide with the luminol analogue L-012. *Free Radic Biol Med* 36:101–111.
- Edwards BS, Bologa C, Young SM, Balakin KV, Prossnitz ER, Savchuck NP, Sklar LA, and Oprea TI (2005) Integration of virtual screening with high-throughput flow cytometry to identify novel small molecule formylpeptide receptor antagonists. *Mol Pharmacol* 68:1301–1310.
- Fiorucci S, Santucci L, Gerli R, Brunori PM, Federici B, Ugolini F, Fabbri C, and Morelli A (1997) NSAIDs upregulate B_2 -integrin expression on human neutrophils through a calcium-dependent pathway. *Aliment Pharmacol Ther* 11:619–630.

- Fletcher S, Steffy K, and Averett D (2006) Masked oral prodrugs of toll-like receptor 7 agonists: a new approach for the treatment of infectious disease. *Curr Opin Investig Drugs* 7:702–708.
- Gauss KA, Bunker PL, Larson TC, Young CJ, Nelson-Overton LK, Siemsen DW, and Quinn MT (2005) Identification of a novel tumor necrosis factor α -responsive region in the NCF2 promoter. *J Leukoc Biol* 77:267–278.
- Gavins FN, Yona S, Kamal AM, Flower RJ, and Perretti M (2003) Leukocyte antiadhesive actions of annexin 1. *Blood* 101:4140–4147.
- Geiszt M, Szeberényi JB, Káldi K, and Ligeti E (1999) Role of different Ca^{2+} sources in the superoxide production of human neutrophil granulocytes. *Free Radic Biol Med* 26:1092–1099.
- Guner O, Clement O, and Kurogi Y (2004) Pharmacophore modeling and three dimensional database searching for drug design using catalyst: recent advances. *Curr Med Chem* 11:2991–3005.
- Guo RF and Ward PA (2005) Role of C5a in inflammatory responses. *Annu Rev Immunol* 23:821–852.
- Hart PH, Spencer LK, Nulsen MF, McDonald PJ, and Finlay-Jones JJ (1986) Neutrophil activity in abscess-bearing mice: comparative studies with neutrophils isolated from peripheral blood, elicited peritoneal exudates, and abscesses. *Infect Immun* 51:936–941.
- Jackson JK, Tudan C, and Burt HM (2000) The Involvement of phospholipase C in crystal induced human neutrophil activation. *J Rheumatol* 27:2877–2885.
- Kenny MT, Balistreri FJ, and Torney HL (1992) β -Lactam antibiotic modulation of murine neutrophil cytokinesis. *Immunopharmacol Immunotoxicol* 14:797–811.
- Klein SM, Cohen G, and Cederbaum AI (1981) Production of formaldehyde during metabolism of dimethyl sulfoxide by hydroxyl radical generating systems. *Biochemistry* 20:6006–6012.
- Labro MT (2000) Interference of antibacterial agents with phagocyte functions: immunomodulation or “immuno-fairy tales”? *Clin Microbiol Rev* 13:615–650.
- Li W and Chung SC (2003) Flow cytometric evaluation of leukocyte function in rat whole blood. *In Vitro Cell Dev Biol Anim* 39:413–419.
- Lundqvist H and Dahlgren C (1996) Isoluminol-enhanced chemiluminescence: a sensitive method to study the release of superoxide anion from human neutrophils. *Free Radic Biol Med* 20:785–792.
- Mathieu MC, Sawyer N, Greig GM, Hamel M, Kargman S, Ducharme Y, Lau CK, Friesen RW, O'Neill GP, Gervais FG, et al. (2005) The C3a receptor antagonist SB 290157 has agonist activity. *Immunol Lett* 100:139–145.
- Nanamori M, Cheng X, Mei J, Sang H, Xuan Y, Zhou C, Wang MW, and Ye RD (2004) A novel nonpeptide ligand for formyl peptide receptor-like 1. *Mol Pharmacol* 66:1213–1222.
- Nemeikaite-Ceniene A, Imbrasaitė A, Sergejdiene E, and Cenas N (2005) Quantitative structure-activity relationships in prooxidant cytotoxicity of polyphenols: role of potential of phenoxyl radical/phenol redox couple. *Arch Biochem Biophys* 441:182–190.
- Nemeth K, Furesz J, Csikor K, Schweitzer K, and Lakatos S (2002) Luminol-dependent chemiluminescence is related to the extracellularly released reactive oxygen intermediates in the case of rat neutrophils activated by formyl-methionyl-leucyl-phenylalanine. *Haematologia* 31:277–285.
- Nicklaus MC, Wang SM, Driscoll JS, and Milne GWA (1995) Conformational changes of small molecules binding to proteins. *Bioorg Med Chem* 3:411–428.
- Petkovic M, Vocks A, Schiller J, and Arnhold J (2005) Oxidative activity of human polymorphonuclear leukocytes stimulated by the long-chain phosphatidic acids. *Physiol Res* 54:105–113.
- Pillai AD, Rani S, Rathod PD, Xavier FP, Vasu KK, Padh H, and Sudarsanam V (2005) QSAR studies on some thiophene analogs as anti-inflammatory agents: enhancement of activity by electronic parameters and its utilization for chemical lead optimization. *Bioorg Med Chem* 13:1275–1283.
- Scheffer J, Knoller J, Cullmann W, and König W (1992) Effects of cefaclor, cefetamet and Ro 40–6890 on inflammatory responses of human granulocytes. *J Antimicrob Chemother* 30:57–66.
- Schiller M, Metze D, Luger TA, Grabbe S, and Gunzer M (2006) Immune response modifiers—mode of action. *Exp Dermatol* 15:331–341.
- Tian S-S, Lamb P, King AG, Miller SG, Kessler L, Luengo JJ, Averill L, Johnson RK, Gleason JG, Pelus LM, et al. (1998) A small, nonapeptidyl mimic of granulocyte-colony-stimulating factor. *Science (Wash DC)* 281:257–259.
- Tomhave ED, Richardson RM, Didsbury JR, Menard L, Snyderman R, and Ali H (1994) Cross-desensitization of receptors for peptide chemoattractants—characterization of a new form of leukocyte regulation. *J Immunol* 153:3267–3275.
- Widdowson KL, Elliott JD, Veber DF, Nie H, Rutledge MC, McClelland BW, Xiang JN, Jurewicz AJ, Hertzberg RP, Foley JJ, et al. (2004) Evaluation of potent and selective small-molecule antagonists for the CXCR2 chemokine receptor. *J Med Chem* 47:1319–1321.
- Witko-Sarsat V, Rieu P, Descamps-Latscha B, Lesavre P, and Halbwachs-Mecarelli L (2000) Neutrophils: molecules, functions and pathophysiological aspects. *Lab Invest* 80:617–653.
- Zahler S, Kowalski C, Brosig A, Kupatt C, Becker BF, and Gerlach E (1997) The function of neutrophils isolated by a magnetic antibody cell separation technique is not altered in comparison to a density gradient centrifugation method. *J Immunol Methods* 200:173–179.
- Zalavary S and Bengtsson T (1998) Modulation of the chemotactic peptide- and immunoglobulin g-triggered respiratory burst in human neutrophils by exogenous and endogenous adenosine. *Eur J Pharmacol* 354:215–225.
- Zhelev DV and Alteraifi A (2002) Signaling in the motility responses of the human neutrophil. *Ann Biomed Eng* 30:356–370.

Address correspondence to: Dr. Mark T. Quinn, Veterinary Molecular Biology, Montana State University, Bozeman, MT 59717. E-mail: mquinn@montana.edu